



Influence of Rotary Assisted Electrical Discharge Machining of 17-4PH Stainless Steel Using Taguchi Technique

Murahari Kolli^{a*}, Satyanarayana Kosaraju^b, Devaraju Aruri^c, & Medikonda Nageswararao^d

^aLakireddy Bali Reddy College of Engineering, Mylavaram 521 230, India

^bGokaraju Rangaraju Institute of Engineering and Technology, Hyderabad 500 090, India

^cKakatiya Institute of Technology and Science, Warangal 506 015, India

^dKoneru Lakshmaiah Education Foundation, Vaddeswaram 522 302, India

Received: 9 September 2022; Accepted: 17 October 2022

The current investigation has study the material removal rate, surface roughness and electrode wear rate in rotary tool assisted EDM of 17-4 PH stainless steel. 17-4 PH SS has widely used in aerospace, marine, nuclear, and chemical processing due to their characteristic high strength to weight ratio and corrosion resistance properties. This paper primarily focuses on enhancing the flushing efficiency of dielectric fluid in the EDM process and to improve the machining performance characteristics. A custom designed rotating electrode attachment has fabricated and used to assist with the EDM process. The experiments are designed and planned using Taguchi L₂₇ Orthogonal array technique. The experiments are planned for four input factors and each parameter is varied at three levels. Current, pulse on time, pulse off time and Electrode Rotation Speed are input factors. ANOVA test is conducted to find out the significance of factors and their percentage contribution on the performance characteristics like Material Removal Rate, Surface Roughness and Electrode Wear Rate. The results concluded that Electrode Rotation Speed has more influence on Material Removal Rate and Electrode Wear Rate. An individual percentage and interaction percentage of parameters from ANOVA confirm that their effects are higher in Material Removal Rate (MRR) compared to Surface roughness (Ra) and Electrode Wear Rate (EWR). Finally, surface morphology studies revealed that significantly less cracks and voids had formed on the EDM'ed sample at optimum condition.

Keywords: Rotary EDM, Taguchi Method, Surface Morphology, PH 17-4 Stainless steel, ANOVA analysis

1 Introduction

Precipitation hardened (PH) Stainless Steels (SS) area class of prominent materials that are widely used in various industries like aerospace, marine, nuclear, chemical processing and medical apparatus due to their exceptional properties such as high strength, high work hardening, high temperature resistance, excellent corrosion resistance and great ductility. The significance of these materials is their ability of bearing very high loads and perform well under heavy machinery services which led to a more widespread usage of these materials in aerospace components. 17-4 PH SS exhibit poor machinability due to their inherent properties; causing in crease in their production cycle time and it is difficult to produce the desired shape and size through traditional machining processes in these materials¹⁻⁷. Adopting conventional methods to machine 17-4 PH SS is highly complicated⁸⁻⁹. To overcome this machining problem,

Unconventional Machining Techniques (UMT) are widely considered for machining of 17-4 PH SS. The Electrical Discharge Machining (EDM) is one of the UMT, which is widely accepted in many manufacturing sectors for electrically conductive materials irrespective of their hardness and strength.

In EDM process, electrical energy is converted into thermal energy through a series of discharge electrical energy pulses supplied to the work piece that leads to melting of mass of material by heat energy generated by the bombardment of electrons through the discharge gap in the submerged dielectric fluid on to the machining surface. During this process, some of the melted material is not flushed away and get deposited on the electrodes surfaces and machined area. These effects are amplified due to insufficient flushing at the spark gap and lower dispersion of energy, abnormal discharges that occur frequently in the machining zone; which ultimately results in lower Material Removal Rate (MRR), Higher Tool Wear Rate (TWR), Enlarged Heat Affected Zone (HAZ),

*Corresponding author (E-mail: kmhari.nitw@gmail.com)

and degraded Surface Finish (Ra). Irregularities such as micro cracks, porosity form on the machined surface due to these effects. To solve these problems, a hybrid UMT EDM process known as Rotary tool assisted EDM (REDM) is used. The REDM process uses a rotating electrode tool as opposed to linearly moving electrode. The rotating electrode working phenomena enhances the centrifugal force of the dielectric fluid, generates a whirl condition for dielectric resulting in uniform mixing thus increasing flushing efficiency, stabilizes the arcing, maintains a uniform discharge energy and efficiently removes the sediment particles resulting in improved machining performance characteristics and effectively mitigates the surface defects and improves wear and fatigue strength of machined surface.

Numerous studies were performed directed at enhancing the machining performances of 17-4 PH SS like MRR, Ra, and EWR of 17-4 PH SS by EDM, few of the researchers concentrated on EDM & hybrid EDM techniques like EDM⁸⁻⁹, PMEDM¹⁰ and WEDM¹⁴. Etemadi A.R et al. examined the metallurgical analysis of crack initiation of Wire-EDM'ed 17-4 PH SS. It is observed that micro cracks are observed while fatigue working on splines after machining¹⁴. Y. Fukuzawa et al. investigated surface modification of SS material with EDM process. They concluded that the modified surface component depends on electrode polarity, work atmosphere, Current (I_p), Pulse-On-Time (T_{on}) and duty factor. It was observed that good carriage and wear resistance is obtained using chromium and sialon electrode tool¹⁵. Abhay K. Jha et al noticed that superior Ra and less micro cracks and White Layer Thickness (WLT) are obtained when powders are added to dielectric fluid in EDM of 15-5 PH SS¹⁶. Chandramouli and Eswaraiah studied optimization of EDM process parameters in machining of 17-4 PH SS using Taguchi method. The EDM process parameters like I_p , T_{on} , Pulse-Off-Time (T_{off}) and Tool Lift Time (Tlt) on the responses like MRR and Ra. The result confirmed that higher MRR and lower Ra values are obtained at higher level conditions of I_p and T_{on} ¹⁷. Subramanian and Thiagarajan investigated the effect of electrode materials on EDM of 316L and 17-4PH SS. The study determines that higher MRR was obtained using copper electrode (Cu), lower TWR and good dimensional accuracy was found for copper-tungsten (W-Cu) electrode¹⁸.

Vikram Reddy et al. studied the influence of surfactant and Gr powder concentration on EDM of

PH17-4 SS. It was reported that addition of Gr particles into dielectric fluid increases dielectric conductivity. As a result, relay time of discharge is shortened and an increase in MRR is achieved. It was also concluded that powder concentration has less effect on all characteristics namely MRR, Ra, SCD and WLT¹⁰. Aliakbari and Baseri investigated the optimization of machining parameters of REDM process by Taguchi method. Electrical parameters and non-electrical parameters were considered as input parameters on their responses TWR, Ra and MRR. They found that the geometry of electrode, rotational speed exhibits discernable effects on the MRR and EWR. The geometry of the electrode has more influence on the flushing quality through rotating electrode machining¹⁹. Priyaranjan Sharma et al. examined EDM of AISI329 SS using Cu and brass (Br) rotary tubular electrode. Taguchi method was used to find out the individual parameters on MRR and TWR. It was revealed that, Cu electrode gives higher MRR and lower TWR rate compared to the Br electrode²⁰.

Muthuramalingam and Mohan²¹ considered the influence of discharge current pulse on machinability in EDM. Taguchi method was used to conduct the experiments on AISI 202SS. Conventional and modified pulse generators were used for doing the experiments, the results were observed to have resulted in more MRR and less Ra. RC-circuit relaxation pulse generator and transistor pulse train generator was considered. It indicated that the ISO current pulse generator obtained less Ra and more MRR compared with conventional generators.²¹ Amandeep Singh and Ranjit Singh examined the effect of PMEDM on various materials with different powders. They concluded that addition of powder particles in dielectric fluid increases MRR and decrease TWR. I_p , T_{on} and powder concentration were found to play an important role on performance characteristics namely MRR, Ra and TWR²². Reza Teimouri and Hamid Baseriv studied the effect of rotational electrode and rotational magnetic field on MRR and Ra. It was observed that three energy levels of electrodes and magnetic fields influenced the MRR and Ra²³. Soni and Chakaravathi investigated the machining characteristic of titanium with REDM. Flushing, electrodes, and motions of the tool electrodes were selected as input parameters and the hole geometry and accuracy were selected as output measures. It can be observed that MRR increase with rotary tool speed and also due to more flushing action

and spark efficiency occurring at the machining zone²⁴.

Throughout the literature study, it was observed that some of the researchers concentrated on several of kinds of materials with different approaches. From the literature, scarce work has been carried out on the influence of RAEDM performance characteristics on PH 17-4 SS with eco-friendly dielectric fluid. Novelty of the present study is to ascertain effects on Ra, EWR and MRR with selecting the eco-friendly dielectric fluid and rotating electrode tool on 17-4 PH Sth it has not been worked yet.

2 Materials and Methods

In the current study, 17-4 PH SS (density 7.8 g/cm³, melting temperature 1404-1440⁰C, Thermal conductivity 19.5 W/m-K) of 75*30*5 mm thickness and electrolyte copper of 70 mm length and 12 mm diameter are considered as the workpiece and electrode materials.

The experiment tests are conducted on the EDM machine attached with a rotary tool electrode. The rotary tool assembly component is attached to the ram part (vertical reciprocating component) of the X-Pert 3-axis EDM machine (Make: Electronica machine tool, Pvt.Ltd, Model: X Pert PS 50 CNC) with E Pulse 50 CNC generator. The rotary assembly component consists of various parts like long and short sheets, DC motor (0-900 rpm), Speed regulator, V-pulley, V-belt, long and short shafts, tool holder, big and small bearings. The shaft rotates at various speeds and feeds downward direction perpendicular to the workpiece component. The E-Pulse 50 CNC generator helps to control the gap voltage and discharge gap. Drinking water is selected as the dielectric fluid of the machining. The workpiece was submerged completely into eco-friendly dielectric fluid (water), half of the tool sank the tank during the machining.

REDM input factors such as I_p, T_{on}, T_{off} and Electrode Rotation Speed (ERS) influence the performance characteristics of 17-4 PH SS. Hence, in this investigation these four input factors are chosen, and other input factors are fixed. The pilot experiments were conducted by selecting input factors to follow the one at a time approach. The corresponding differences were measured on the MRR, Ra and EWR. Based on pilot experimental results, three levels of the four factors are selected for the study. The input factors and their ranges are illustrated in Table 1.

Table 1 — Rotary assisted EDM input factor and ranges

Symbol	Parameters	Units	Level 1	Level 2	Level 3
A	Current (Ip)	Amp	10	15	20
B	Pulse on time(Ton)	µs	30	50	75
C	Pulse off time Toff)	µs	20	25	30
D	Electrode rotation speed (ERS)	RPM	250	400	580

A total of 27 experiments are conducted using Taguchi L₂₇ Orthogonal Array (OA) technique and their performance results are shown in Table 2. All the experiments were conducted on the 17-4 PH SS and constant time was maintained between each experiment. MRR and EWR are calculated using electronic weighing balance(Make: Citizen Model CY204). At the initial stage of every experiment, the top and bottom surfaces of electrode are cleaned; to eliminate the unwanted particles. The MRR and EWR performance factors values are calculated by using Equation 1 and 2, respectively.

$$MRR = \frac{\text{(Weight before machining–after machining)} \times 1000}{\text{Density} \times \text{Experiment time}} \dots(1)$$

$$EWR = \frac{\text{(Weight before machining–after machining)} \times 1000}{\text{Density} \times \text{Experiment time}} \dots(2)$$

Handysurf (Make: ZIESS Model E-35B) surface tester was used to measure the EDM’ed samples Ra at five distinct locations and the average value is noted. After conducting experiments, the machined samples are cut the cross section using WEDM process. For SEM analysis the samples are prepared using polishing operation to remove the effect of WEDM process. To measure the recast layer thickness, the 17-4 PH SS specimens are polished with various grade emery papers. Further, the samples are polished by diamond polishing using alumina diamond paste. The properly polished specimens are etched with HCL, acetic acid and HNO₃. The rotary EDMed experimental samples are presented in Fig. 1.

2.1. Planning of experiments based on Taguchi’s Method

Taguchi’s technique is a famous tool for design of experiments to deal with response performance characteristics influenced by the machining input parameters. It is a simple, efficient and systematic technique to find out the best input factors. It’s an influential tool that substantially decreases the number of experiments needed to create models and



Fig. 1 — Experimental samples.

improves the performance characteristics. It saves a significant amount of time and cost in planning of experimental designs. The Taguchi technique is to support the optimization of process and then determination of best conditions of performance characteristics of EWR, Ra and MRR.

The experimental values of EWR, Ra and MRR responses are subsequently transferred to signal to noise (S/N) ratio. In the present study the EWR and Ra responses are “lower the better” values and MRR response is “higher the better” values. Further, it uses the experimental results to convert the S/N ratio values to mean values to measure the deviation of the response from the mean value. S/N ratio for “Higher the Better” and “Lower the Better” performance characteristics are calculated by adopting the Equation 3 and 4, respectively.

$$\eta = -10 \log_{10} \left[\frac{1}{n} \sum_{i=1}^n \frac{1}{y_i^2} \right] \quad \dots(3)$$

$$\eta = -10 \log_{10} \left[\frac{1}{n} \sum_{i=1}^n y_i^2 \right] \quad \dots(4)$$

Where, y_i is the experimental run value of the i^{th} experiment and “ n ” is the total number of experiments, and “ η ” denotes the S/N ratio of converted values. Using MINITAB 17.0 software is considered to design and analyze experimental data. There are four input factors and three levels are considered in the investigation. All four factors have different degrees of freedom. As a result, $L_{27}(3^4)$ OA is chosen. Each experiment run is repeated three times in order to reduce the noise/error effect. The performance characteristics of Ra, EWR and MRR of

Table 2 — L_{27} Orthogonal array layout and experimental values

Expt No	A (Ip)	B (Ton)	C (Toff)	D (ERS)	MRR (mm^3/min)	SR (μm)	EWR (mm^3/min)
1	10	30	20	250	25.7815	4.54	0.5075
2	10	30	25	400	28.8284	4.48	0.7258
3	10	30	30	580	29.9534	4.39	1.1027
4	10	50	20	400	27.5803	5.12	2.012
5	10	50	25	580	28.9484	4.94	1.9861
6	10	50	30	250	32.8992	5.13	2.1146
7	10	75	20	580	32.026	5.19	2.2518
8	10	75	25	250	34.2196	5.23	1.4412
9	10	75	30	400	36.0235	4.91	1.5145
10	15	30	20	400	30.7553	4.39	3.177
11	15	30	25	580	31.4797	4.56	3.2585
12	15	30	30	250	38.649	4.47	1.9727
13	15	50	20	580	31.6516	5.12	3.2372
14	15	50	25	250	42.4258	5.27	2.3751
15	15	50	30	400	32.2825	4.91	2.4852
16	15	75	20	250	42.7862	5.52	1.7465
17	15	75	25	400	36.4965	5.21	3.5745
18	15	75	30	580	32.3017	4.98	2.1678
19	20	30	20	580	38.8629	4.78	3.2915
20	20	30	25	250	45.235	5.65	2.1391
21	20	30	30	400	42.1492	5.47	1.4485
22	20	50	20	250	48.0968	5.76	1.794
23	20	50	25	400	41.1472	5.99	2.783
24	20	50	30	580	43.524	5.53	2.1833
25	20	75	20	400	44.953	6.23	4.6521
26	20	75	25	580	43.1297	6.16	5.1026
27	20	75	30	250	49.9857	6.12	4.7548

PH-17-4 SS are calculated for all the trails. The significance input factors influences on the characteristics are verified using the ANOVA. Finally, optimum condition of the Ra, EWR and MRR values are calculated.

3 Results and Discussion

In this section the influence of input factors considering I_p , T_{on} , T_{off} and ERS on the performance factors selecting MRR, Ra and EWR of the 17-4PH SS is studied. The experimental runs and results of performance characteristics values are presented in Table 2.

3.1 Influence of input factors on MRR

The influence of input factors on MRR; S/N ratio response plot and ANOVA table are given in the Fig. 2 and Table 3. Figure 3 shows the influence of input factors on MRR. From the 2D response plot for S/N ratio, it was identified that there is an increase in MRR gradually with the increase in the I_p from 10A

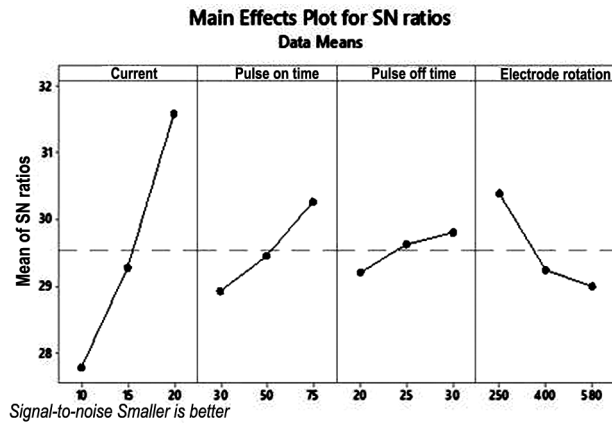


Fig 2 — SN Ratio plot MRR

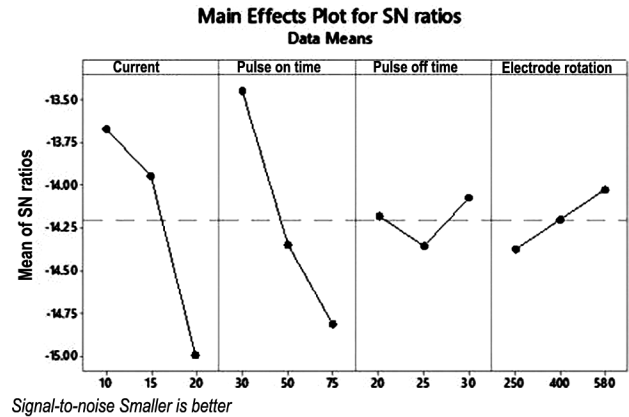


Fig. 3 — SN Ratio plot of SR.

Table 3 — ANOVA results of MRR

Source	F	Seq SS	Adj MS	F	P	%
Ip	2	46.1181	23.059	357.84	0	68.49
Ton	2	5.5102	2.755	42.75	0	8.18
Toff	2	1.0854	0.542	8.42	0.018	1.61
ERS	2	7.14	3.57	55.4	0	10.6
Ip*Toff	4	2.1425	0.535	8.31	0.013	3.18
Ip*ERS	4	4.0549	1.013	15.73	0.002	6.02
Error	10	1.2803	0.64			1.92
Total	26	67.331				100

to 20A i.e., as shown in the Fig. 2. The highest value of current generates more current densities, results in high thermal energy production in the machining zone, it results in increase in the MRR¹³. It can be observed from the Fig. 2 there is an increase in MRR with increase of T_{on}. With increasing T_{on} from 30µs to 75µs plasma channel becomes wider and more energy concentrates on the work surface. Due to the availability of increased amount of heat generated in the working gap results in huge amount of material being melted. From the Fig. 2, an increase in MRR is observed as the T_{off} which is increased from 20µs to 30µs due to removing the unwanted particles on the both material and electrode surfaces and to produce more ions transformation to next spark initiation. The trend can be depicted from the Fig. 2 of the MRR verses ERS. According to the figure the MRR values is decreasing with an increase in the ERS. When the ERS is set at 250 rpm, MRR approached the maximum value, and further increasing the ERS gradually decreases the MRR.

The MRR mathematical model generated using the Minitab 17.0 software. The mathematical equation is useful in predicting the performance characteristic of MRR. The equation is developed as the mathematical

relationship of input factors on the performance factors. The MRR mathematical Equation (5) is expressed as

$$\begin{aligned}
 \text{MRR} = & 12.2 + 0.65I_p + 0.144T_{on} + 1.05T_{off} - \\
 & 0.0542ERS + 0.0793I_p * I_p + 0.00023T_{on} * \\
 & T_{on} - 0.0079T_{off} * T_{off} + 0.000074 \\
 & ERS * ERS - 0.00459I_p * T_{on} - 0.0325I_p * T_{off} - \\
 & 0.001554I_p * ERS \dots(5)
 \end{aligned}$$

The input factors effecting the MRR can be observed from ANOVA tables for S/N ratios as shown in the Table 3. The important observations are found on the table from P-values, F-values and % contributions of the input factors. The P-values which are greater than 0.05 indicates that the model terms are significant. In this MRR model I_p, ERS, T_{on} and T_{off} are the most significant terms. The value of R² and R²(pred) for MRR models are 98.6% and 94.1% respectively. Hence, the MRR optimum condition is obtained at A3B3C3D1. It has been confirmed that higher values of I_p(20A), T_{on}(75µs), and T_{off}(30µs) and lower values of ERS (250rpm) provided the maximum MRR value at 49.6549 mm³/min. Finally, it can be concluded that enhancing discharging sparking, current intensity, on time and off time in the rotation tool, MRR increases.

3.2 Influence of input factors on Ra

The ANOVA results of Ra values are indicated in the Table 4 and corresponding S/N ratio response graphs are depicted in Fig. 3. From the response plots of Ra as shown in the Fig. 3, it was observed that Ra increases with increase in I_p from 10A to 20 A. The increase in Ra value is due to the high amount of spark energy released in the spark gap and as a result, this causes a huge amount of electrons bombarding the material leading to wider and deep craters to occur

Table 4 — ANOVA results of SR

Source	DF	Seq SS	Adj MS	F	P	%
Ip	2	9.2962	4.648	182.7	0	40.77
Ton	2	8.7191	4.3595	171.35	0	38.24
ERS	2	0.5706	0.2853	11.21	0	2.5
Ip*Ton	4	1.2627	0.3156	12.41	0.009	5.53
IP*Toff	4	1.2451	0.3112	12.23	0.005	5.46
Ip*ERS	4	1.1944	0.2985	11.74	0.005	5.26
Error	8	0.5097	0.2548			2.24
Total	26	22.797				100

in the machined surface eventually degrading the surface finish³. From Fig. 3, it can be concluded that when T_{on} increases from $30\mu s$ to $75\mu s$, Ra increases because, high discharge energy is supplied to the material surfaces for more amount of time, which led to the formation of large voids and cracks. As shown in the Fig. 3, when T_{off} increases from 20 to $30\mu s$, there is a decrease in Ra since increasing T_{off} leads to uniform heat loss and provides more time to flush away the debris in the machining zone. This leads to drop in temperature of the workpiece surface before the next spark occurs, thus reducing the crater size and improving the Ra. It is noticed that Ra increases with increase in the ERS from 250 to 580 rpm and is depicted in the Fig. 3. When ERS is low, there is a provision of large number of sparks to be produced in the spark gap and a single discharge spark period is sufficient for the spark to reach the surface of machined area thus producing uniform craters and voids producing better surface finish.

The Ra mathematical model is given as Equation 6. Equation 6 is developed as the mathematical relationship for input factors on the Ra. The Ra mathematical equation (6) is expressed as

$$Ra = 3.26 - 0.427 Ip + 0.0555 Ton + 0.222 Toff + 0.00024 ERS + 0.01502 Ip * Ip - 0.000446 Ton * Ton - 0.00538 Toff * Toff + 0.000001 ERS * ERS + 0.000550 Ip * Ton + 0.00257 Ip * Toff - 0.000074 Ip * ERS \dots (6)$$

An ANOVA result for Ra is observed in Table 4. From the table, it can be observed that the important process parameters are I_p , T_{on} and ERS. The values of R^2 96.6% and adj R^2 91.1%, of the model are within variability range for predicating Ra values. Finally, response plots revealed that at lower conditions of I_p (10A) and T_{on} ($30\mu s$), and higher conditions of T_{off} ($30\mu s$) and ERS (580 rpm) the minimum value of the Ra ($3.65\mu m$) is obtained. The optimum condition

Table 5 — ANOVA results of EWR

Source	DF	Seq SS	Adj MS	F	P	%
Ip	2	125.95	62.974	26.8	0.001	40.93
Ton	2	23.93	11.963	5.09	0.051	7.77
Toff	2	24.25	12.125	5.16	0.05	7.88
ERS	2	18.25	9.124	3.88	0.083	5.94
Ip*Ton	4	52.09	13.021	5.54	0.032	16.93
IP*Toff	4	24.35	6.087	2.59	0.143	7.92
Ip*ERS	4	24.75	6.188	2.63	0.139	8.05
Error	6	14.1	2.35			4.58
Total	26	307.66				100

of the Ra ($A_1B_1C_3D_3$) is indicated at the lowest levels of input parameters.

3.3 Influence of input factors on EWR

In EDM machining of components, maintained precision and accuracy are important; it depends on the electrode material and properties. Electrode wear is significant response characteristic involved on the selection of EDM factors and ranges. This discusses the influence of input factors on EWR. Table 5 represents the ANOVA Table for EWR. It is observed that a significant effect is caused by I_p , Ton and ERS on EWR. Figure 4 shows the response plot of EWR versus input factors. Fig. 4 depicts that the value of EWR tend to decrease with I_p to a minimum value i.e., at 10A after that it gradually increases. When the sparks occur, only few electrons strike on the electrode surface rather than on the part, thus resulting in a lower amount of material removed from the electrode. From Figure 4, it can be understood that the EWR increases with increasing the Ton from $30\mu s$ to $75\mu s$. When the Ton is $75\mu s$, more time is spent on ionizing the discharge gap, causing an increased rate of burning and evaporation of material on electrodes. In the same way, it can be observed from the Fig. 4, EWR decreases with increasing the Toff from $20\mu s$ to $30\mu s$. When the Toff is $30\mu s$ sufficient time is available to cool the material surface and for cleaning of the electrodes surfaces. Quenching effect is also occurring on the electrodes surface hardened the material surfaces results in very less wear is occurring. In contrast it can be observed from Fig. 4 that EWR decreases with increasing the ERS from 250 to 580 rpm. When the ERS is 580 rpm, electrons movement and energy transformation are lower on the discharge gap which causes lower material melting and vaporization are occurred. This causes lower EWR at 250 rpm of electrode because it frequently allows a huge amount of dielectric fluid in

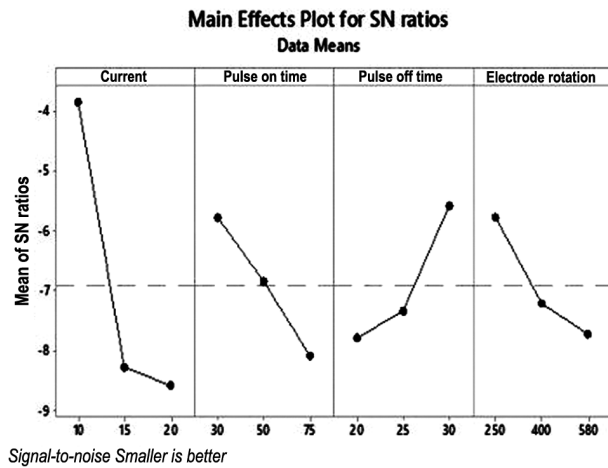


Fig. 4 — SN Ratio plot of EWR.

Table 6 — Optimum conditions and confirmations

Performance characteristics	Optimum condition	Optimum value	Experimental value
MRR (mm ³ /min)	A ₃ , B ₃ , C ₃ , D ₁	50.77	49.98
SR (µm)	A ₁ , B ₁ , C ₁ , D ₃	4.31	4.39
EWR (mm ³ /min)	A ₁ , B ₁ , C ₃ , D ₁	0.677	0.713

the discharge gap, destabilize the spark discharges there by increasing the MRR.

The EWR mathematical model relating input and output characteristics is shown in Equation 7. The equation is useful in predicting the performance characteristic on EWR material. The EWR mathematical equation (Eq 7) is expressed as

$$\begin{aligned} \text{EWR} = & -8.57 + 0.709 I_p - 0.1218 T_{on} + 0.596 T_{off} + \\ & 0.00470 ERS - 0.02593 I_p * I_p + 0.000806 T_{on} \\ & * T_{on} - 0.01197 T_{off} * T_{off} - \\ & 0.000009 ERS * ERS + 0.003710 I_p * T_{on} - \\ & 0.00505 I_p * T_{off} + 0.000333 I_p * ERS \dots(7) \end{aligned}$$

In this EWR model I_p , T_{on} and ERS are most significant input factors. The value of R^2 and R^2 (pred) for EWR models are 97.4% and 92.6% respectively. Finally, the EWR best condition is obtained at $A_1B_1C_3D_1$. It is concluded that at minimum EWR of 0.677 is found at the lowest levels of I_p (10A), T_{on} (30µs), and T_{off} (30µs), and ERS (250 rpm).

3.4 Conformation of experiments

The confirmation experiments are the concluding stages to be verified for the mathematical development of performance characteristics namely MRR, Ra and EWR. Table 6 shows the optimum condition value and experimental value for the best

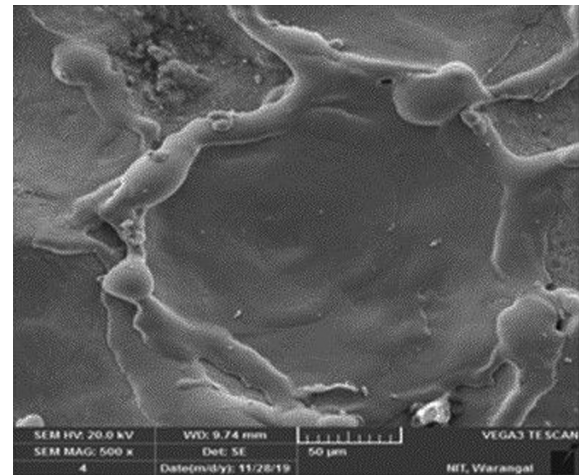


Fig 5 — Surface morphology analysis

conditions of REDM of 17-4 PH SS alloy. The experimental results are indicated and confirm that the optimal parameters conditions for MRR i.e $A_3B_3C_3D_1$, $Rai.eA_1B_1C_1D_3$ and $EWRi.eA_1B_1C_3D_1$ give best performances. The percentage of error between experimental and predicted values for performance characteristics lies within 6.60%, 3.28% and 3.68%, for MRR, Ra and EWR respectively, it indicated the Table 6.

3.5 Surface morphology

Surface morphology of 17-4 PH SS EDM'd samples are observed in Fig. 5. The SEM analysis confirmed the presence of various surface structures, voids, water droplet craters globule of debris, and accumulated debris particles. Figure 5 surface texture was deteriorating due to the high influence on the I_p , and T_{on} . When the I_p and T_{on} are increased the surface texture of the EDM'd sample was observed to have various sizes of overlapping craters, deep voids, and debris. The deep voids and overlapping craters were generated because of series of discharges, extreme heat, melting and evaporation of the workpiece material. The higher I_p effect, regularly cracking of dielectric fluid results in a high amount of material bombardment and huge tensile forces. Hence, these causes degrade the surface finish. Lower I_p and T_{on} influences less discharge energy produced in the material surface causing less material melt and evaporation. This effect forms uniform craters, less voids and small droplet marks found on the EDM'd surface results in superior surface finish.

4 Conclusion

The electrode rotation influence on MRR, Ra and EWR of the REDM process was successfully

implemented on 17-4 PH SS, the following conclusions can be made:

- It is found that best MRR was obtained at A₃B₃C₃D₁ condition and experimental value is 49.98 (mm³/min), higher I_p and lower ERS are more influential on the MRR.
- The optimum Ra is observed at A₁B₁C₁D₃ condition, and the result value is 4.39 (μm), lower I_p, T_{on} and higher ERS effect on the Ra.
- The optimum EWR is indicated at A₁B₁C₃D₁ condition and the result value is 0.713 (mm³/min), lower I_p, T_{on} and higher ERS influenced on the Ra.
- The Ra sample surface morphology observed that uniform distribution of craters, less voids and micro cracks were formed on the EDM'ed sample.
- Conformation results of optimum and experimental conditions values are within the ranges, MRR at 50.77 to 49.98 (mm³/min), Ra at 4.31 to 4.39 (μm) and EWR at 0.667 to 0.713 (mm³/min).

Acknowledgment

The authors appreciate the facilities provided by the Central Institute of Plastic and Engineering Technology (CIPET) Lucknow, National Institute of Technology (NIT) Warangal and KLEF vaddeswaram.

References

- 1 Chien W T, & Tsai C S, *J Mater Process Technol*, 140 (2003) 340.
- 2 Raj SV, Ghosn LJ, Lerch BA, Hebsur M, Cosgriff LM, & Fedor J, *Mater Sci Eng A*, 456 (2007) 305.
- 3 Arisoy CF, Başman G, & Şeşen MK, *Eng Fail Anal*, 10 (2003) 711.
- 4 Bhaduri AK, Gill TP, Srinivasan G, & Sujith S, *Sci technol weld joining*, 4 (1999) 295.
- 5 Lin X, Cao Y, Wu X, Yang H, Chen J, & Huang W, *Mater Sci Eng A* 553 (2012) 80.
- 6 Wu JH, & Lin CK, *Metall Mater Trans*, 33 (2002) 1715.
- 7 Akita M, Uematsu Y, Kakiuchi T, Nakajima M, & Kawaguchi R, *Mater Sci Eng: A*, 666 (2016) 19.
- 8 Chandramouli S, & Eswaraiiah K, *Mater Today: Proc*, 5 (2018) 5058.
- 9 Reddy VV, Valli PM, Kumar A, & Reddy CS, *J Adv Manuf Syst*, 14 (2015) 189.
- 10 Reddy VV, Kumar A, Valli PM, & Reddy CS, *J Braz Soc Mech Sci Eng*, 37 (2015) 641.
- 11 Kolli M, & Kumar A, *Eng Sci Technol Int J*, 18 (2015) 524.
- 12 Kolli M, & Kumar A, *Proc Inst Mech Eng, Part B: J Eng Manuf*, 231 (2017) 641.
- 13 Kolli M, & Kumar A, *Silicon*, 11 (2019) 1731.
- 14 Etemadi AR, Fazel B, & Emami A, *J fail anal prev*, 11 (2011) 493.
- 15 Fukuzawa Y, Kojima Y, Tani T, Sekiguti E, & Mohri N, *Mater Manuf Process*, 10 (1995) 195.
- 16 Jha AK, Sreekumar K, & Sinha PP, *Eng Fail Anal*, 17 (2010) 1195.
- 17 Chandramouli S, & Eswaraiiah K, *Mater Today: Proc*, 4 (2017) 2040.
- 18 Gopalakannan S, & Senthilvelan T, *J Miner Mater Charact Eng*, 11 (2012) 685.
- 19 Aliakbari E, & Baseri H, *Int J Adv Manuf Technol*, 62 (2012) 1041.
- 20 Sharma P, Singh S, & Mishra DR, *Procedia Mater Sci*, 5 (2014) 1771.
- 21 Muthuramalingam T, & Mohan B, *Mater Manuf Processes*, 28 (2013) 375.
- 22 Singh A, & Singh R, *Int J Innov Res Sci Technol*, 2 (2015) 164.
- 23 Teimouri R, & Baseri H, *Int J Adv Manuf Technol*, 67 (2013) 1371.
- 24 Soni JS, & Chakraverti G, *Wear*, 171 (1994) 5.